water

MDPI

Communication

Study on the Effect of Water Flux in Osmotic Microbial Fuel Cells on Membrane Water Content and Resistance

Yang Zhao [1,2,3], Yonghui Song [1,3,*] and Liang Duan [1,3,*]

[1] State Key Joint Laboratory of Environment Simulation and Pollution Control, School of Environment, Tsinghua University, Beijing 100084, China; zhaoyang@craes.org.cn
[2] State Key Laboratory of Environmental Criteria and Risk Assessment, Chinese Research Academy of Environmental Sciences, Dayangfang 8, Anwai Beiyuan, Beijing 100012, China
[3] Research Department of Basin Water Environmental Governance, Chinese Research Academy of Environmental Sciences, Dayangfang 8, Anwai Beiyuan, Beijing 100012, China
* Correspondence: songyh@craes.org.cn (Y.S.); duanliang@craes.org.cn (L.D.)

Abstract: Osmotic microbial fuel cells (OsMFCs) can integrate forward osmosis into microbial fuel cells (MFCs), which are able to perform organic elimination, bioenergy production, and high-class water abstraction from wastewater. However, it is not well understood how the unique feature of OsMFCs, i.e., water flux, helps improve current generation. Based on experimental studies and the Springer model theory, a new method for representing water transmission in OsMFC membranes is put forward that considers water transmission by electro-osmosis resulting from proton flux through the membrane and by osmosis resulting from osmotic pressure grades of water. In this research, osmotic water transmission is associated with the permeable differential pressure resulting from the ionic differential concentration in the membrane, and electro-osmotic water transmission is found to be proportional to the current density employed but irrelevant to the composition gradients. The net water transmission in OsMFC depends on the operation time and increases accordingly with higher current density and composition gradients. Furthermore, the membrane's proton conductibility and water-transmission capabilities are significantly affected by the moisture content, which decreases from the negative electrode to the positive electrode in the OsMFC system. Increasing water flux with higher osmotic pressure and current density is therefore able to diminish the resistance of the membrane.

Keywords: water transmission; electro-osmosis; osmosis; water content

check for updates

Citation: Zhao, Y.; Song, Y.; Duan, L. Study on the Effect of Water Flux in Osmotic Microbial Fuel Cells on Membrane Water Content and Resistance. *Water* **2022**, *14*, 848. https://doi.org/10.3390/w14060848

Academic Editors: José Antonio Mendoza-Roca and Amparo Bes-Piá

Received: 9 February 2022
Accepted: 7 March 2022
Published: 9 March 2022

1. Introduction

Forward osmosis (FO) membranes are regarded as an innovative technology, and they have recently attracted increasing attention in the areas of effluent disposal and recycling [1]. Due to the use of the driving power of osmotic pressure instead of hydraulic pressure, FO membranes can obtain pure water, which is higher in quality because of its high retention rate of various pollutants. Although MFCs can effectively handle a wide range of pollutants and produce bioelectricity without the need for energy from power systems, the waste of MFCs cannot be used to achieve direct emissions or reutilization without further disposal [2]. Therefore, the quality of the wastewater for the further utilization of MFCs must be promoted in the course of wastewater disposal. To enhance the rate of water recovery in MFCs, OsMFCs were exploited by integrating FO with MFCs. For OsMFCs, an FO membrane, rather than CEM, is applied for the purpose of separating the positive electrode and the negative pole, and this semipermeable membrane can only pervade the proton from high to low water potential when driven by a permeable differential pressure [3]. The diversity of traditional MFCs means that OsMFCs are able to distill high-quality water from the anolyte, including wastewater, by utilizing an FO membrane. Furthermore, OsMFCs are able to produce more electricity in interrupted and

continuous modes by utilizing saline or synthetic sea water as the catholyte [4]. Although the utilization of FO membranes can produce more electricity than the application of CEM, the reason remains unknown. Generally speaking, the properties of MFCs are influenced by its intrinsic loss, such as ohmic loss and density loss [5]. In particular, by substituting CEM with an FO membrane, one might influence the resistance of the membrane, the pH discrepancy in the catholyte and the anolyte, and the spread of oxygen. It is also important to understand how water flux affects power production, which is a phenomenon unique to OsMFCs. According to one report, based on the polarization curve, it can be found that the internal resistance of the air–cathode OsMFC is low compared to MFCs that contain CEM or AEM, which might result from the promotion of ion delivery because of water flux [6]. Proton migration could also be accelerated by water flux, in which case the increase in the catholyte pH and reduction in the anolyte pH declines [7].

Since the forward osmosis membrane is the separator material of OsMFCs, its conductivity has an important impact on the properties of OsMFCs. Research reports have confirmed that the membrane's moisture content and water distribution determine its conductivity, since water is used as the carrier of the proton transfer in the forward osmosis membrane, and protons are transmitted from the positive electrode to the negative electrode in the form of form hydrated protons [8]. The higher the water content of an FO membrane, the more uniform the water distribution and the faster the proton conduction rate in the membrane. Therefore, the study of water distribution is of great significance to improve the performance of OsMFCs. It is impossible for FO membranes to deliver ions selectively, which is not the case for CEM. Nevertheless, the unique characteristic of OsMFCs, i.e., water flux, has been found to be helpful in promoting generating capacity [9]. The mechanisms of water transmission in membranes include water flux taking place in an electric field produced by the interaction between protons and water molecules (electro-osmotic drag), permeation produced by pressure gradients, and chemical or Fickian spread resulting from the grades of the water's chemical activity [10]. For OsMFCs, these grades lead to a water flux back towards the positive electrode, which is an excessive imposition on the water flux.

To increase our understanding of improved electricity production in OsMFCs, in this study, we used the Springer model theory [11] to consider the factors affecting the water content in the membrane, including pressure, temperature, and electric field. Specifically, in an OsMFC system, the driving force of water migration in the membrane mainly comes from the electric field and the osmotic pressure difference. Densities of different draw solutions that are unequal between the two sides lead to chemical voltage grades on the membrane, which produce ionic distribution and osmotic water transmission. As is the case for all electrochemical systems, water transmission can occur because of osmosis or electro-osmosis [12], as shown in Figure 1. Based on the model put forward by Gierke et al., at first [13], a low moisture content is achieved at the positive electrode of an OsMFC, which can result in small hydrophilic clusters. Furthermore, the stress produced by the water cluster and applied on the water in the cluster is relatively small. However, for the negative electrode of the membrane, the higher the water absorption, the larger the inflation of the hydrophilic domains [14].

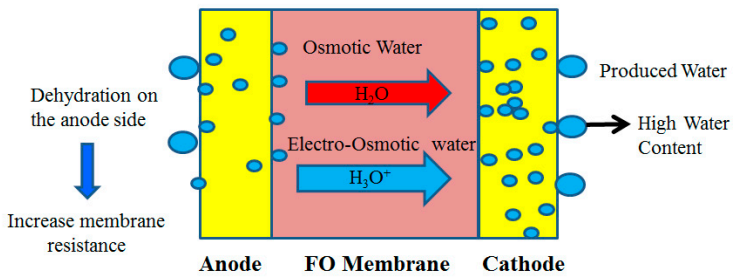

Figure 1. Water transmission in a forward osmosis microbial fuel cell.

The literature points out that on the microcosmic scale, so-called 'homogenous' ion exchange membranes are uneven in space, which influences the membranes' capabilities [15]. This is referred to as the microinhomogeneity of the membrane. According to a previous investigation [16], the membrane can be separated into two stages. Phase 1 consists of a gel-like phase, which includes an electric polymer matrix with settled ionic groups, as well as an electric solution of movable counterions that is able to offset the electricity of the substrate. Phase 1 also contains membrane reinforcements or inert fillers in the polymer. Phase 2 is described as an electrically neutral solution, which is found in constructional cavities or at the heart of the larger centers of expanded membranes. The ionic groups have a low concentration, and the contractibility of the molecules in the clustered water is relatively high. We believe reverse transmission is guided by grades with such a shape in a flexible main chain, which is regarded as grades of permeable stress with negative values [17].

Consequently, the key mechanism of water transmission in OsMFCs includes forward transport caused by driving forces from gradients in osmotic pressure and electric field, as well as back transport of the convective flux caused by the negative permeable stress grades. These water transport mechanisms significantly affect the membrane's conductivity, and we therefore investigated them to deepen our understanding. However, it must be remembered to that it is currently difficult to accurately quantify such mechanisms due to the simultaneous influence of various factors. The specific objectives of this research were to (1) investigate osmotic and electro-osmotic water transmission in OsMFCs, (2) demonstrate the effect of current density and osmotic pressure difference on water content, and (3) analyze the effect of current and osmotic pressure on water content and membrane resistance.

2. Materials and Methods

2.1. OsMFC Setup and Operation

The OsMFC was made up of two partitions of the same size (250 mL), i.e., the positive and negative electrode, which were divided by an FO membrane. The FO membrane unit, which had an available membrane area of 32 cm^2, was manufactured with sulfonated polyphenylene sulfone (sPPSU) (Aquaporin, Copenhagen, Denmark). Before it was used, the TFC membrane was immersed in deionized (DI) water for half an hour based on the producer's recommendation. Two carbon brushes (Sanye Carbon Co., Beijing, China) were preconditioned by immersing them in pure acetone for one night, after which heat treatment was performed in an electric muffle at 450 °C for 30 min; after preconditioning, they were intercalated into the positive electrode partition to form the positive electrodes. The negative electrode was a sheet of carbon cloth covered with platinum (Pt) as the activator to perform the oxygen reduction reaction (0.3 mg Pt cm^{-2}).

The OsMFC was operated at a room temperature of ~21 °C, and the germ mud was obtained from a local effluent-disposal factory (Qinghe Effluent Disposal Factory, Beijing, China). The positive electrode was supplemented with an acetic acid solution that included (per L of DI water): sodium acetate, 1 g; NH_4Cl, 0.15 g; NaCl, 0.5 g; $MgSO_4$, 0.015 g; $CaCl_2$, 0.02 g; $NaHCO_3$, 0.1 g; KH_2PO_4, 0.53 g; K_2HPO_4, 1.07 g; and trace element, 1 mL. The OsMFC directly utilized the compounded liquid in the bioreactor as an inoculant and groundmass. When the electricity was constant, the OsMFC startup was considered complete.

2.2. Analytical Methods

The water permeation flux (J_s, Lm^{-2} h^{-1}, abbreviated as LMH) is calculated using Equation (1) [18].

$$J_s = \frac{\Delta V}{A_s \Delta t} \tag{1}$$

where ΔV (L) is the infiltration water, which is obtained during the reserved time Δt (h), i.e., the period of the experiment; and A is the available membrane surface size (m^2).

Water transport experiments were performed under a regime of different osmotic pressures and constant current. Four different concentrations of draw solutions were used to measure osmotic water transport (1 M, 1.5 M, 2 M, and 2.5 M NaCl) and were kept in an open circuit. To measure electro-osmotic transport, different ampere densities were employed and were adjusted to 1, 5, 12, and 15 A m^{-2} by varying external resistance. Electro-osmotic water transport number, t_w (mol H_2O/H^+), and osmotic water were determined at different NaCl concentrations and at different applied currents. All displayed tests were repetitive and carried out more than once.

Water transmission was determined in the course of OsMFC with a current density between 1 and 15 A m^{-2} by keeping the draw solution at 1 M. By continuously measuring the mass of the recircular bottles, the increase in catholyte mass could be determined. Water transmission can be divided into (1) osmotic water transmission and (2) electro-osmotic water transmission. No water losses were detected during the experiments. Therefore, in the course of the OsMFC tests, the variation in the weight of the losses resulted from osmosis and electro-osmosis. The permeable flow could be measured by turning of the cycle of electricity.

To determine the membrane resistance, a six-partition cell with a permutation of four electrodes was applied, as shown in Figure S1. The central membrane, which was the membrane used in the research, was a forward osmosis membrane and was counterweighed in the solution for at least 24 h. A 0.5 M measure of NaCl was pumped as far as both partitions next to the membrane being studied. The middle partition included the same liquid in order to avoid the impact of the half reaction. The pole partitions contained a 0.5 M Na_2SO_4 solution. The positive electrode partition included a positive electrode that was manufactured with titanium coated with platinum. The negative electrode partition included a negative electrode that was manufactured with stainless steel. Cogwheel pumps were utilized to pump the liquids. The conductivity and pH of the liquid near the membrane being studied were examined constantly to ensure that the composition remained constant throughout the tests. All tests were carried out at a temperature of 25 °C. A power source was linked to the positive electrode and the negative electrode to allocate electricity to the six-partition cell. A power supply was connected to the anode and the cathode to apply the current over the six-compartment cell. Haber–Luggin capillaries were used as electrodes. These capillaries were filled with the same solution (and same concentration) as that present in the specific compartment, and they were connected to a small reservoir containing Ag/AgCl reference electrodes. The ultimate resistance was determined by detecting the gradient of the current density versus the electric tension decline curve, which represents the jointed liquid and resistance of the membrane:

$$R_m = \frac{U}{i} \tag{2}$$

where U is the voltage drop determined between the Haber–Luggin capillaries (V), and i is the current density (A m^{-2}).

Water content, λ, is given as the specific value of the quantity of hydrons with respect to the quantity of electricity ($SO_3^-H^+$) locations. The moisture content of the membrane was determined by weighing 20 forward membranes with a balance according to the serial number as the thickness was increased to 0.1 cm. To determine the water content of the membrane, 20 membranes were stacked to increase the film thickness to 0.1 cm, and the membranes, which were wet, were abstracted from the OsMFC, after which the spare water on the surface was quickly removed using paper towels. Then, the wet membranes were weighed (mi, g). After the treatment with cryodesiccation for one night, they were weighed (mj, g) again. Thus, the moisture content is determined by the formula $m_1 - m_2$ (g).

3. Results and Discussion

3.1. Water Transport

3.1.1. Osmotic and Electro-Osmotic Water Transport in OsMFCs

Since OsMFC is a technology that is utilized to dispose of different pollutants and produce bioelectricity, it does not need to consume electricity. With the transport of protons, water is also transported, and the density distribution of the membrane is affected by water transmission [19]. Water transmission can take place with free (osmosis) or bound (electro-osmosis) water. The first form especially occurs when there are large osmotic pressure differences because of the difference in density adjacent to the membrane (see Equation (6)) [20]. In the context of OsMFCs, the delivery of water bound to protons is called electro-osmosis [21], which occurs when the protons are going through the membrane [22].

In the course of OsMFC power generation, electric osmosis may result in a large amount of water transmission through ionic exchange membranes [23]. Water is then inevitably transmitted through the membrane by the means of osmosis and electric osmosis, which play a significant role in the conductibility of the membrane. The amount of water that is delivered differs between membranes, but it is affected first by the moisture content and extrinsic salt density and subsequently by temperature and the settled electric density [24]. Furthermore, the depth of the membrane might also influence the inner concentration distribution, which is important to study because the depth of the membrane is often decreased in order to lower the drag force of the membrane.

3.1.2. Measured Osmotic Water Transport

Osmotic water transmission is associated with osmotic stress diversity resulting from the ionic density difference on the membrane. The quantity of water transmitted by osmosis, Δm (mol), can be determined by utilizing the following formula:

$$\Delta m = D_{\mathrm{w}} \frac{A(C_{\mathrm{c}} - C_{\mathrm{a}})}{\delta} t \tag{3}$$

where D_{w} is the permeable water-delivery coefficient ($\mathrm{m^2\ s^{-1}}$); A is the membrane size ($\mathrm{m^2}$); C_{a} and C_{c} are the concentration of the anolyte and catholyte ($\mathrm{mol\ m^{-3}}$), respectively; δ is the membrane depth (m); and t is time (s). The determined permeable water transmission is displayed in Figure 2. Using the data collected, the permeable water-delivery coefficient (D_{w}) of the membrane was assessed by utilizing Equation (3) and the curve of regression shown in Figure 2. The regression coefficient of this line is equal to D_{w} over δ in Equation (3). The membrane depth, δ, is taken as the mean membrane depth of the FO membranes (50×10^{-6} m), which leads to the result that $D_{\mathrm{w}} = 5.38 \times 10^{-8}\ \mathrm{m^2\ s^{-1}}$. This is shown to be one order of scale lower than the distribution coefficient of water placed in a true solution.

It is well known that water-delivery parameters are largely dependent upon water absorption because of sorption. Figure S2 displays a diagrammatic sketch of the device to measure the water transport number, t_{H2O}. The membrane separates two compartments containing 2 g/L synthetic wastewater (NaAc) and NaCl solution, and it is sustained with grids from the two sides. Protons are delivered from the positive to the negative electrode partition. Water transported by electro-osmotic drag causes an increase in catholyte volume and a decrease in anolyte volume, which is measured by calibrated capillaries. The water transport number was determined by making the outcomes of the positive and the negative electrode partitions equal. The measurement continued until the change in volume was 0.01 mL for both partitions.

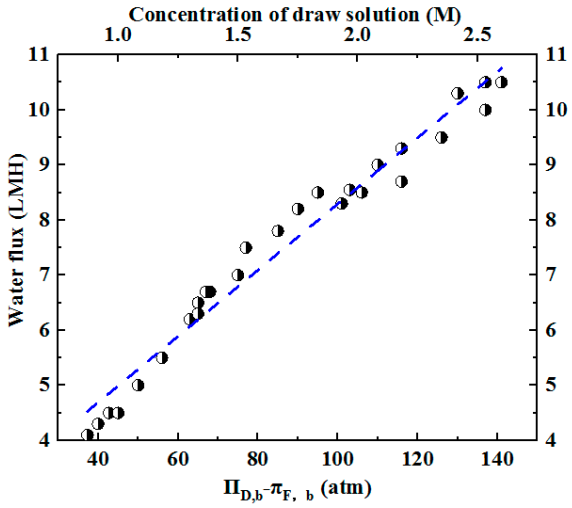

Figure 2. Osmotic water flux determined under diverse NaCl density (M) differences between the catholyte and anolyte (dotted line) based on linear Equation (3).

3.1.3. Measured Electro-Osmotic Transport

Net electro-osmotic water transport, $\nabla m_{\text{e-osm}}$ (mol), is calculated using Equation (4):

$$\nabla m_{\text{e-osm}} = t_{\text{w}} \frac{jA}{z_i F} \nabla t \tag{4}$$

in which t_{w} is the water transport quantity, j is the employed current density (Am^{-2}), z_i is the electrovalency, and F is the Faraday (Cmol^{-1}). For OsMFCs, the electro-osmotic water transmission into the membrane can be determined according to the proton flux passing through the membrane, which is given by the particular current density and the water transmission quantity based on the moisture content.

$$J_{\text{H}_2\text{O}}^{\text{EO}} = \frac{t_{\text{H}_2\text{O}} i}{F} \tag{5}$$

The water transport number can be formulated as:

$$t_{\text{H}_2\text{O}} = \frac{J_{\text{H}_2\text{O}}}{J_{\text{H}^+}} \tag{6}$$

The electro-osmotic water transmission, J_{H2O}, is confirmed to be the water transmission determined during a certain duration minus the mean permeable delivery at the start and end of that duration. The final electro-osmotic water transport number is displayed in Figure 3, which shows that the water transmission drops as the current density increases and reaches the limit when the current density is moderate. Only a few researchers have considered the influence of water transmission on current density. For example, Tombalakian et al. indicated that [25] water transmission values drop when the current density is high. They pointed out that this is associated with the polarization that occurs when the ampere densities are high. When the current density is less than 1.076 Am^{-2}, the membrane has no effect on the water transmission current density. The water transmission determined for 1 mA current density in this research (shown in Table 1) is likely to sustain this finding. Lakshminarayaniah [26] indicated that electro-osmotic delivery increases when the ampere densities are small and drops when the ampere densities are large. Furthermore, at higher current densities, water transport approaches an extreme point, which mainly results from the uneven charge division in sol layers of the pore liquid. In the context of low electricity, sol layers in the heart of the pores are movable, whereas the extreme point is generated for water transmission when there is a large amount of electricity. The data acquired in this research also prove this point. In the present research, the electro-osmotic water

transmission number was found to be proportional to the current density employed and irrelevant to the composition gradient. The mean water transmission quantity, t_w, of the membrane was shown to be 40 (±1.5) mol H_2O/H^+. This quantity is much higher than that of other membranes because numerous investigators studied electro-osmotic water transmission by introducing ion exchange membranes at extrinsic NaCl densities in the scope (0.5–2.5 M) [27], probably due to the high water flux of forward osmotic membranes.

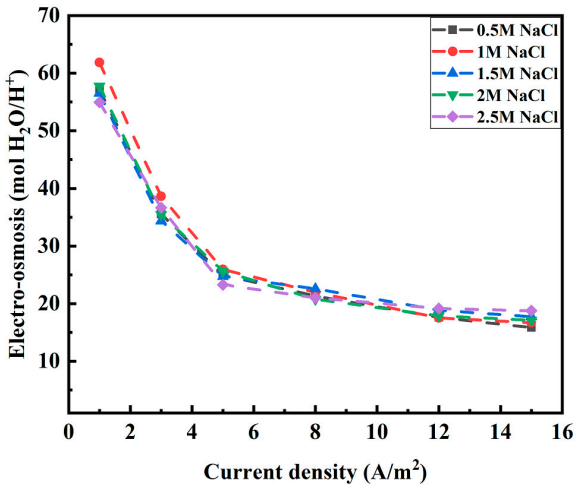

Figure 3. Electro-osmotic water-delivery quantity, t_w (mol H_2O/H^+) measured at different NaCl density differences and at various ampere densities.

Table 1. Water-delivery data for NaCl of various densities.

Current Density A/m^2	Moles of Water Transported per Mole of Protons Delivered				
	0.5 M	1 M	1.5 M	2 M	2.5 M
1	57.12	61.86	56.52	57.76	54.95
3	35.52	38.63	34.37	35.45	36.64
5	24.92	25.93	24.73	25.62	23.25
8	21.32	21.97	22.57	20.76	21.00
12	17.60	17.52	18.87	17.86	19.15
15	15.83	16.68	17.72	17.11	18.75
	Moles of water transported per Faraday of current passed				
1	235.80	218.80	216.80	213.00	231.20
3	127.93	133.60	101.80	110.73	127.10
5	75.72	71.58	66.39	69.07	72.07
8	63.78	62.39	57.85	87.99	58.02
12	53.13	56.04	45.39	50.85	50.71
15	47.96	46.30	43.30	47.62	46.75

3.1.4. Higher Water Transport at Lower Current Density

Since water transmission may influence the concentration profile in the membrane and the membrane conductivity [28], understanding osmotic and electro-osmotic water transmission quantities can allow us to offer helpful input arguments for the modeling of OsMFCs. This chart can be further interpreted using measurements of osmosis and electro-osmosis. Osmotic water transmission is based on the duration of conduction and therefore increases as the current density declines and the composition gradients increase. The water transmission through the FO membrane utilized in this research was modeled using the values that were obtained through D_w and t_w. All the water transmission and the osmotic portions are displayed in Figure 4. When the ampere densities are less than 4.86 Am^{-2}, electropermeable water transmission through the membrane exceeds the osmotic water due to electro-osmosis.

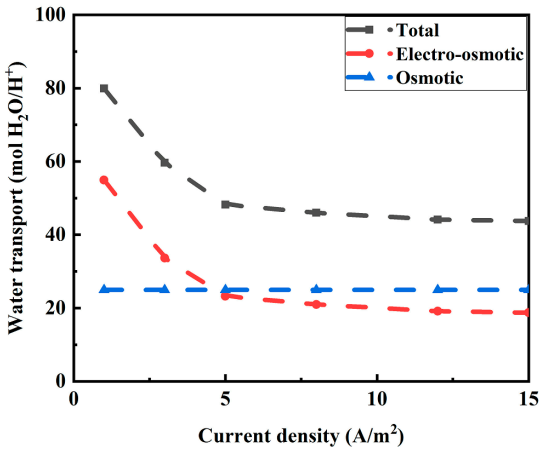

Figure 4. Calculated delivered water (mol/H^+) based on the values of t_w and D_w determined in this research as a function of the employed current density.

3.2. Water Content

3.2.1. The Effect of Current Density on Water Content

Figure 5a displays water distribution as a function of the depth determined from the negative electrode, on the left, across from the FO membrane (50 µm) when there are four ampere densities. The net water flux ratio, β, of the current density of the 0.2 A cm^{-2} curve is 19 water molecules per H^+ ion delivered through the membrane, as shown in Figure 5b. When the current density is high, there is a large amount of net water flux, even if the rate of net water flux of each proton is small; therefore, at the negative electrode, the values range from 14.1 to 15 when the current density increases from 0.1 to 0.8 A cm^{-2}. The slope of the water profiles declines from the negative to the positive electrode, which is mainly because the resistance flux is proportional to the moisture content, and thus, less distribution flux is needed to counteract it at a stable condition nearer to the positive electrode.

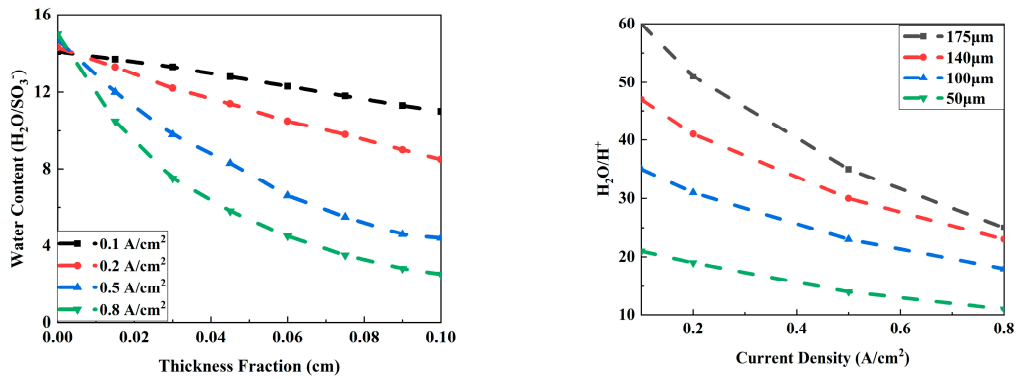

(**a**) (**b**)

Figure 5. Water profiles in the FO membrane for four ampere densities when catholyte concentration is kept continuous at 35 g L^{-1} NaCl. The positive electrode is on the left, whereas the net water flux moves from right to left (**a**). H_2O/H^+ flux-specific value, β, vs. current density of four FO membrane thicknesses when the catholyte concentration is kept constant at 35 g L^{-1} NaCl (**b**).

3.2.2. The Effect of Osmotic Pressure on Water Content

Figure 6a displays that the osmotic pressure on both sides of the membrane had a larger impact on the water content, as well as the division, for the FO membrane. Moisture content on the negative electrode reached 25 when the osmotic pressure difference was 106 atm, whereas it was only 15 at the maximum current density. Meanwhile, due to the osmotic pressure, water in the membrane moved from the feed to the draw solution,

resulting in a rapid decrease in moisture content at the positive electrode. When the osmotic pressure difference was kept at a low level (43 atm), the moisture content in the negative electrode end stayed above 15, and the water distribution in the membrane was relatively uniform. When the osmotic pressure increased, there was more moisture content in the negative electrode end, reaching 27 at 137 atm and higher net water flux at 10.6 LMH. However, there was more serious dehydration on the anode side, decreasing to less than 2 at the 0.1 cm position of the membrane.

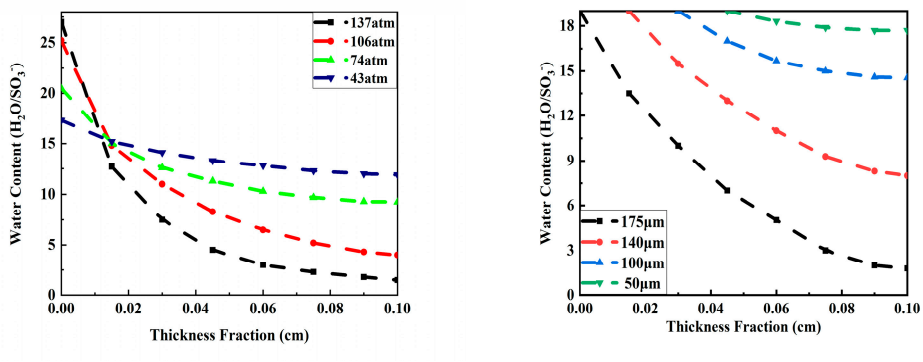

(**a**) (**b**)

Figure 6. Water profiles in the FO membrane for four osmotic pressures when the circuit was held open. The negative electrode is on the left, and the net water flux moves from right to left (**a**). Profiles of the membrane water content for different membrane thicknesses (**b**).

3.2.3. Water Content of Different Membrane Thicknesses

Four membrane thicknesses were compared when the current density of the OsMFC was 0.2 Am^{-2} and the osmotic pressure was 43 atm. Figure 6b shows that the higher the membrane depth, the more permeable the back delivery of the water is. This leads to superproportional growth of the ohmic wastage as the membrane depth increases. We can conclude that as far as the membrane is concerned, the moisture content varies with position such that it is the highest at the cathode side and the lowest at the anode side. Moreover, the stronger the applied current density or osmotic pressure difference, the more non-uniform the division of the moisture content is. Therefore, FO membranes with different thicknesses have different distributions of water content and were selected to investigate the effect of the membrane thickness on the membrane resistance and potential. It is important to investigate this because a decrease in the depth of membrane reduces the resistance of the membrane.

3.3. Membrane Resistance

The conductibility of the membrane is derived from ions located in the moving phase. Low extrinsic density leads to high swelling, as well as a large moving phase. Furthermore, low extrinsic density causes conductibility to decline, as the density is based on the amount of extrinsic liquid. As Zabolotsky et al. indicated [29], the microarchitectural unevenness of the membrane is the major reason for the dependence of the density on the conductibility, which shows that microcavities and microchannels [30] can affect the conductivity of the membrane. This finding shows that the membrane follows an intrinsic density distribution with mainly low density, and it presents a dramatic growth in density towards a high concentration.

This density distribution can be interpreted as being caused by water transmission from low to high salinity and by NaCl delivery to the reverse orientation. Equation (3) indicates that permeable capability is based on the difference in salt density between extrinsic liquids. When the circuit situation is open, permeation occurs in the reverse direction to ion distribution, i.e., from low to high. The intrinsic distribution coefficient of water is shown to be one order of scale larger than that of salt [31]. Therefore, a

spreading water flux passing through the membrane may lead to a dramatic distribution of density [32]. This finding proves that there is an obvious increase in membrane conductance as the moisture content increases.

3.3.1. Effect of Membrane Thickness on Membrane Resistance and Voltage

Membranes with low electricity have a moisture content close to 14 water molecules in depth and a resistance below 0.2 Ω cm^2, as shown in Figure 7. The addition of water by reducing the membrane thickness enhances the capability of the cell by significantly reducing the resistance. The initial H_2O/H^+ flux ratio, β, of a 50 μm membrane was about 23 at 0.1 A cm^{-2}, but it reached 52 for a 175 μm membrane because the difference in the thickness between the positive electrode and negative electrode presents a grade that is the same as the membrane moisture content. It is impossible for a thicker membrane to deliver a large amount of water to the positive electrode, which leads to a decrease in λ, principally because the resistance coefficient is proportional to λ. This causes a decrease in electro-osmotic resistance, as well as an increase in the resistance, which illustrates that thinner membranes can have proper moisture content, as well as uniform distribution throughout a membrane. Meanwhile, the quantity of hydrons delivered per proton increases the power of the denser membranes while decreasing the current density, which means that a higher depth results in a decreased permeable back delivery of water, as well as a more powerful dehumidification at the positive electrode end. This leads to the superproportional growth of the ohmic depletion as the membrane depth grows.

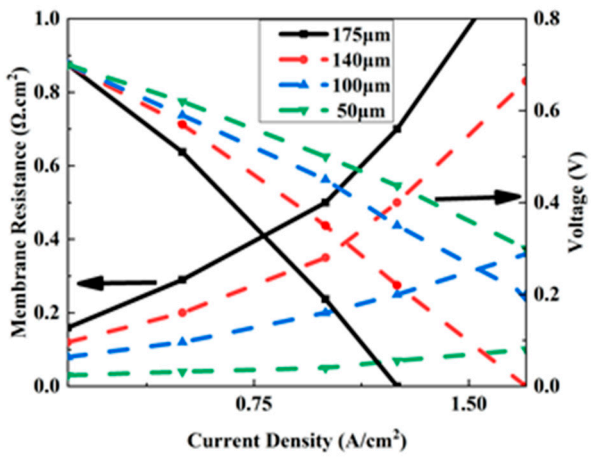

Figure 7. Cell voltage and membrane resistance vs. current density for different membrane thicknesses with catholyte concentration held constant at 35 g L^{-1} NaCl.

3.3.2. The Effect of Current and Osmotic Pressure on Membrane Resistance and Water Flux

Due to the electro-osmotic effect, the current density of the OsMFC is considered a crucial moving force for water delivery, and its effect was examined under the conditions of a closed circuit and an open circuit. In the conditions of a 117.6 Ω extrinsic resister and 43 atm osmotic pressure, current density was proven to be 1.8 A m^{-2}. The water flux and membrane resistance were 5.3 LMH and 25 Ω cm^2, respectively. In contrast, when the circuit situation was open, the OsMFC could not produce any electricity, with 5.0 LMH water flux and 89 Ω cm^2 membrane resistance.

Further comparison was conducted by examining other extrinsic resistance values in order to determine the relationship between water flux, current generation, and membrane resistance in OsMFCs. This relationship was investigated at a settled catholyte NaCl concentration of 1 M (43 atm). Thus, the extrinsic resistance was found to be different for an open circuit with 117.6 Ω, which represents the production of a different amount of electricity. As anticipated, current density grew from 0.05 Am^{-2} to 1.8 Am^{-2} when the extrinsic resistance dropped from 2358 Ω to 117.6 Ω. Water flux increased from 5.1 to

5.3 LMH when current generation was increased, with the membrane resistance dropping from 89 Ω cm^2 to 25 Ω cm^2.

Water flux is significant in OsMFCs, as it influences water purification and electricity production. To study the influence of water flux, we studied the membrane resistance at different osmotic pressures. To achieve the same electricity production, five current densities (including an open circuit) in four osmotic pressure conditions were created; the ampere densities under such situations were similar at 1.8, 0.7, 0.12, and 0.05 A m^{-2}, as shown in Figure S3. Nevertheless, they showed diverse water flux values, i.e., 5 LMH at 43 atm osmotic pressure with an open circuit and 11.3 LMH at 137 atm at the same current density. When current density was increased to 1.8 Am^{-2} and osmotic pressure was increased to 137 atm, the water flux increased to 13 LMH. This demonstrates that the current density and osmotic pressure were able to increase water delivery from the anode liquid to the cathode liquid, as shown in Figure 8.

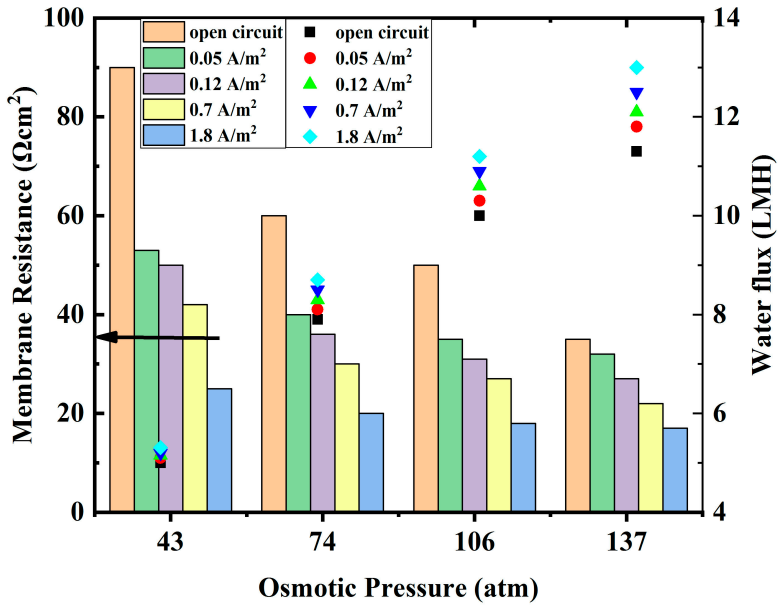

Figure 8. The effect of current and osmotic pressure on membrane resistance and water flux.

4. Conclusions

This research has revealed that the membrane resistance of OsMFCs is influenced by membrane thickness and by water delivery. Water delivery takes place under both osmosis and electro-osmosis conditions. This study found electro-osmotic water transmission to be in proportion to the current density that was applied and irrelevant to the composition gradient. When a low current density was employed, an electro-osmotic water transmission lower than 4.86 A m^{-2} was able to surpass osmotic water transmission due to electro-osmosis. An increase in water flux on the membrane (high osmotic pressure and low current density) decreases the membrane's resistance. The amount of water is affected primarily by the water content. Water content in an FO membrane decreases from the negative electrode to the positive electrode end; the higher the osmotic pressure difference and current density, the stronger the influence on the moisture content distribution and the greater the moisture content attenuation on the positive electrode end. Furthermore, the higher the moisture content of an FO membrane, the more uniform the water distribution and the lower the membrane resistance.

Supplementary Materials: The following are available online at https://www.mdpi.com/article/10.3390/w14060848/s1, Figure S1: Six compartment cell used to determine the membrane resistance, Figure S2: Set-up for measurement of the water transport number t_{H2O}, Figure S3 Similar current generation under different conditions (1 M NaCl as catholyte/117.6 Ω external resistance initially and 2.5 M NaCl as catholyte/2358 Ω external resistance finally.

Author Contributions: Conceptualization, Y.Z.; methodology, Y.Z.; software, L.D.; validation, Y.Z.; formal analysis, Y.Z.; investigation, Y.Z.; resources, L.D.; data curation, Y.Z.; writing—original draft preparation, Y.Z.; writing—review and editing, Y.Z.; visualization, Y.Z.; supervision, L.D.; project administration, Y.S. and L.D.; funding acquisition, Y.S. All authors have read and agreed to the published version of the manuscript.

Funding: We offer our appreciation for support of project from the National sewage treatment and control technological special project (2017ZX07401004).

Institutional Review Board Statement: Not applicable.

Informed Consent Statement: Not applicable.

Data Availability Statement: Not applicable.

Conflicts of Interest: The authors declare no conflict of interest.

References

1. Chen, L.; Gu, Y.S.; Cao, C.Q.; Zhang, J.; Ng, J.E.; Tang, C.Y. Performance of a submerged anaerobic membrane bioreactor with forward osmosis membrane for low-strength wastewater treatment. *Water Res.* **2014**, *50*, 114–123. [CrossRef]
2. Zhang, Y.X.; He, W.H.; Ren, L.J.; Stager, J.; Evans, P.J.; Logan, B.E. COD removal characteristics in air-cathode microbial fuel cells. *Bioresour. Technol.* **2015**, *176*, 23–31. [CrossRef]
3. Cath, T.Y.; Childress, A.E.; Elimelech, M. Forward osmosis: Principles, applications, and recent developments. *J. Membr. Sci.* **2006**, *281*, 70–87. [CrossRef]
4. Ge, Z.; Ping, Q.; Xiao, L.; He, Z. Reducing effluent discharge and recovering bioenergy in an osmotic microbial fuel cell treating domestic wastewater. *Desalination* **2013**, *312*, 52–59. [CrossRef]
5. Logan, B.E.; Hamelers, B.; Rozendal, R.; Schröder, U.; Keller, J.; Freguia, S.; Aelterman, P.; Verstraete, W.; Rabaey, K. Microbial fuel cells: Methodology and technology. *Environ. Sci. Technol.* **2006**, *40*, 5181–5192. [CrossRef] [PubMed]
6. Werner, C.M.; Logan, B.E.; Saikaly, P.E.; Amy, G.L. Wastewater treatment, energy recovery and desalination using a forward osmosis membrane in an air-cathode microbial osmotic fuel cell. *J. Membr. Sci.* **2013**, *428*, 116–122. [CrossRef]
7. Zhang, F.; Brastad, K.S.; He, Z. Integrating forward osmosis into microbial fuel cells for wastewater treatment, water extraction and bioelectricity generation. *Environ. Sci. Technol.* **2011**, *45*, 6690–6696. [CrossRef]
8. Eikerling, M.; Kharkats, Y.I.; Kornyshev, A.A.; Volkovich, Y.M. Phenomenological theory of electro-osmotic effect and water management in polymer electrolyte proton-conducting membranes. *J. Electrochem. Soc.* **1988**, *145*, 2648. [CrossRef]
9. Lutchmiah, K.; Verliefde, A.R.D.; Roest, K.; Rietveld, L.C.; Cornelissen, E.R. Forward osmosis for application in wastewater treatment: A review. *Water Res.* **2014**, *58*, 179–197. [CrossRef]
10. Springer, T.E.; Zawodzinski, T.A.; Gottsfeld, S. Polymer electrolyte fuel cells model. *J. Electrochem. Soc.* **1991**, *138*, 2334. [CrossRef]
11. Springer, T.E.; Zawodzinski, T.A.; Wilson, M.S.; Gottesfled, S. Characterization of polymer electrolyte fuel cells using ac impedance spectroscopy. *J. Electrochem. Soc.* **1996**, *143*, 587–599. [CrossRef]
12. Kalogirou, S.A. Seawater desalination using renewable energy sources. *Prog. Energy Combust. Sci.* **2005**, *31*, 242–281. [CrossRef]
13. Gierke, T.D.; Munn, G.E.; Wilson, F.C. The morphology in nafion perfluorinated membrane products, as determined by wide and small angle x-ray studies. *J. Polym. Sci. Pol. Phys.* **1981**, *19*, 1687–1704. [CrossRef]
14. Lu, Y.; Jia, J.; Miao, H.; Ruan, W.; Wang, X. Performance improvement and biofouling mitigation in osmotic microbial fuel cells via in situ formation of silver nanoparticles on forward osmosis membrane. *Membranes* **2020**, *10*, 122. [CrossRef]
15. Kang, M.S.; Choi, Y.J.; Choi, I.J.; Yoon, T.H.; Moon, S.H. Electrochemical characterization of sulfonated poly(aryleneetherulfone)(S-PES) cation exchange membranes. *J. Membr. Sci.* **2003**, *216*, 39–53. [CrossRef]
16. Berezina, N.P.; Kononenko, N.A.; Dyomina, O.A.; Gnusin, N.P. Characterization of ion-exchange membrane materials: Properties vs. structure. *Adv. Colloid Interface Sci.* **2008**, *139*, 3–28. [CrossRef]
17. Długołęcki, P.; Ogonowski, P.; Metz, S.J.; Saakes, M.; Nijmeijer, K.; Wessling, M. On the resistances of membrane, diffusion boundary layer and double layer in ion exchange membrane transport. *J. Membr. Sci.* **2010**, *349*, 69–379. [CrossRef]
18. Wang, K.Y.; Ong, R.C.; Chung, T.S. Double-skinned forward osmosis membranes for reducing internal concentration polarization within the porous sublayer. *Ind. Eng. Chem. Res.* **2010**, *49*, 4824–4831. [CrossRef]
19. Mohamed Berber, R.; Ismail, M.S.; Pourkashanian, M. Mohamed Barakat Zakaria Hegazy. Promising Membrane for Polymer Electrolyte Fuel Cells Shows Remarkable Proton Conduction over Wide Temperature and Humidity Ranges. *ACS Appl. Polym. Mater.* **2021**, *3*, 4275–4286. [CrossRef]

20. Long, C.; Zhao, T.; Tian, L.; Liu, Q.; Wang, F.H.; Wang, Z.H.; Zhu, H. Highly Stable and Conductive Multicationic Poly(biphenyl indole) with Extender Side Chains for Anion Exchange Membrane Fuel Cells. *ACS Appl. Energy Mater.* **2021**, *4*, 6154–6165. [CrossRef]
21. Pham, T.A.; Nam, L.V.; Choi, E.; Lee, M.S.; Jun, T.S.; Jang, S.; Kim, S.M. Mechanically Stable Thinned Membrane for a High-Performance Polymer Electrolyte Membrane Fuel Cell via a Plasma-Etching and Annealing Process. *Energy Fuels* **2021**, *35*, 11525–11532. [CrossRef]
22. Bellows, R.J.; Lin, M.Y.; Arif, M.; Thompson, A.K.; Jacobson, D. Neutron Imaging Technique for In Situ Measurement of water transport gradients within Nafion in Polymer Electrolyte Fuel Cells. *J. Electrochem. Soc.* **2000**, *146*, 1099. [CrossRef]
23. Al-Mamun, A.; Baawain, M.S.; Dhar, B.R.; Kim, I.S. Improved recovery of bioenergy and osmotic water in an osmotic microbial fuel cell using micro-diffuser assisted marine aerobic biofilm on cathode. *Biochem. Eng. J.* **2017**, *128*, 235–242. [CrossRef]
24. Oda, Y.; Yawataya, T. On the electro-osmotic water transport through cation exchange resin membranes. *Bull. Chem. Soc. Jpn.* **1955**, *28*, 263–269. [CrossRef]
25. Tombalakian, A.S.; Barton, H.J.; Graydon, W.F. Electroösmotic water transport across ion-exchange membranes. *J. Phys. Chem. A* **1962**, *66*, 1006–1009. [CrossRef]
26. Lakshminarayaniah, N. Transport Phenomena in Artificial Membranes. *Chem Rev.* **1965**, *65*, 491–565. [CrossRef] [PubMed]
27. Wang, H.; Fu, B.; Xi, J.; Hu, H.; Liang, P.; Huang, X.; Zhang, X. Remediation of simulated malodorous surface water by columnar air-cathode microbial fuel cells. *Sci. Total Environ.* **2019**, *687*, 287–296. [CrossRef]
28. Qin, M.; Ping, Q.; Lu, Y.; Abu-Reesh, I.M.; He, Z. Understanding electricity generation in osmotic microbial fuel cells through integrated experimental investigation and mathematical modeling. *Bioresour. Technol.* **2015**, *195*, 194–201. [CrossRef]
29. Zabolotsky, V.I.; Nikonenko, V.V. Effect of structural membrane inhomogeneity on transport properties. *J. Membr. Sci.* **1993**, *79*, 181–198. [CrossRef]
30. Yaroslavtsev, A.B. Perfluorinated ion-exchange membranes. *Poly. Sci. Ser. A* **2013**, *55*, 674–698. [CrossRef]
31. Veerman, J.; de Jong, R.M.; Saakes, M.; Metz, S.J.; Harmsen, G.J. Reverse electrodialysis: Comparison of six commercial membrane pairs on the thermodynamic efficiency and power density. *J. Membr. Sci.* **2009**, *343*, 7–15. [CrossRef]
32. Spiegler, K.S. Transport processes in ionic membranes. *Trans. Faraday Soc.* **1958**, *54*, 1408–1428. [CrossRef]